NASA TECHNICAL NOTE

NASA TN D-4157

NASA TN D-4157

THEORETICAL PERFORMANCE OF SOLAR-CELL SPACE POWER SYSTEMS USING SPECTRAL DISPERSION

II - Dispersion by Diffraction Gratings

by Thomas M. Klucher

Lewis Research Center
Cleveland, Ohio

NATIONAL AERONAUTICS AND SPACE ADMINISTRATION • WASHINGTON, D. C. • SEPTEMBER 1967

NASA TN D-4157

THEORETICAL PERFORMANCE OF SOLAR CELL SPACE POWER SYSTEMS USING SPECTRAL DISPERSION

II - DISPERSION BY DIFFRACTION GRATINGS

By Thomas M. Klucher

Lewis Research Center
Cleveland, Ohio

NATIONAL AERONAUTICS AND SPACE ADMINISTRATION

For sale by the Clearinghouse for Federal Scientific and Technical Information
Springfield, Virginia 22151 – CFSTI price $3.00

THEORETICAL PERFORMANCE OF SOLAR CELL SPACE POWER SYSTEMS USING SPECTRAL DISPERSION II - DISPERSION BY DIFFRACTION GRATINGS

by Thomas M. Klucher

Lewis Research Center

SUMMARY

Photovoltaic p-n junctions of the single energy band gap type used in planar arrays are limited theoretically to conversion efficiencies less than 30 percent because they cannot utilize the total energy available in the sun's spectrum. Consequently, systems have been devised which attempt to match portions of the sun spectrum with solar cell material for optimum conversion efficiency. This report presents a simplified theoretical analysis of one such system employing concentrating mirrors and diffraction gratings to disperse and to distribute the sun's incident power to a suitable array; the array composed of the semiconductor materials, germanium (Ge), silicon (Si), indium phosphide (InP), gallium arsenide (GaAs), cadmium telluride (CdTe), and gallium arsenide phosphide ($GaAs_{1-x}P_x$), was arranged to convert the sun's energy over the wavelength range 0.3 to 1.5 microns. Two grating configurations in the dispersed light system were studied; one had a concave grating and the other had a plane grating.

This analysis shows that such a system, suffering no losses in the optical system, could exhibit a conversion efficiency which is 1.2 to 1.8 times that attainable from an optimum conventional array throughout the temperature range 0° to 150° C. Reflection and diffraction losses reduce the efficiencies of the dispersed light system considerably. The plane grating configuration shows no advantage over the conventional array. The concave configuration does exceed the theoretical 26-percent conversion efficiency for the conventional array, with theoretical efficiencies of 26 to 35 percent for the dispersed light system at the lowest operating temperatures. Further analysis, involving comparison of power-to-weight ratio between the competing systems, indicates the necessity of very lightweight optical components in the dispersion system; the area density of the concentrating mirror must be about one-half the area density of the photovoltaic array in order to show an advantage in relative power-to-weight ratio. Since the analysis was based on optimistic assumptions concerning the performance of the optical system, efficiencies and power-to-weight ratio of the dispersed light system would suffer further reduction when analyzed under more specific design considerations.

INTRODUCTION

Photovoltaic devices have served usefully as sources of electric power aboard a variety of spacecraft in past years. Requiring only the energy available from the sun, arrays fabricated from these devices are relatively lightweight, are reliable, and, under most environmental conditions, have long lifetimes. They are low-temperature devices, however, and are able to convert only photons with energy greater than their semiconductor band gap energy. Moreover, even those photons having energies greater than the band gap are not converted efficiently; the energy in excess of the band gap is dissipated within the device as useless heat. Photovoltaic cells of the single band gap variety used in present arrays, therefore, are limited theoretically to power conversion efficiencies which are less than 30 percent of the available sunlight power impinging upon their surfaces (ref. 1). If the theoretical efficiency limit of 30 percent is to be overcome, an array would have to include photovoltaic cells which are so arranged that there is a match between photon energy and material band gap throughout the spectral distribution of the sun. The result of such a match would be a greater conversion of the photon flux into useful current carriers with a minimum of heating. Jackson (ref. 2) proposed fabrication of a spectrum matching solar cell, composed of layers of different semiconductor materials, which could have a theoretical efficiency as high as 86 percent. Serious problems relating to construction of these cells arise, however, and none has yet been developed.

Another technique of spectrum matching has been proposed which would employ chromatic dispersion of sunlight. The system basically consists of a concentrating mirror, a dispersing agent, and an array composed of a variety of single-gap photovoltaic cells. The dispersing agent, a diffraction grating in this analysis or a prism in a previous analysis (ref. 3), receives light from the concentrating mirror, reduces the light into chromatically dispersed beams, and focuses the spectrum onto an array of photovoltaic cells. The cells are so arranged according to band gap that they absorb the total photon flux in an efficient manner.

It is the purpose of this study to evaluate the dispersed light system, to estimate the efficiencies and the power-to-weight ratios, and to compare these parameters with those obtained for a conventional array, operating under equivalent white-light illumination. The following approach was taken in the evaluation. An upper limit of efficiency for a dispersed light system with six different single band gap type semiconductors was first computed with no energy losses due to grating diffraction or to system optical elements. The effects of blaze angle in the grating, overlap of diffraction orders, and of surface specular reflection losses were next calculated to estimate efficiency and power-to-weight ratios under more realistic conditions. Because the efficiency of the photovoltaic process is sensitive to the operating temperature, the equilibrium temperatures of both arrays had to be calculated. For the dispersed light system, several equilibrium tem-

peratures dependent on the intensity of light arriving from the concentrating mirror had to be calculated. The conversion efficiencies and the power-to-weight ratios of the dispersed light system were then compared with the efficiency and the power-to-weight ratio of a gallium arsenide planar array, the material which yields optimum theoretical efficiency for conventional arrays.

Thus, the analysis is limited to a brief evaluation of losses expected to occur within individual system components under ideal system conditions. Other important system losses related to defocusing caused by the sun's cone of light, optical surface irregularities, and alinement inaccuracies, as well as detailed inherent imperfections in image formation present in all real optical devices, have not been considered. These losses, of course, would have to be investigated in a more comprehensive study if the analysis presented herein should demonstrate considerable performance advantage of the dispersion system over ordinary planar arrays.

SYMBOLS

A	area of array, m^2
A_m	projected area of concentrating mirror, m^2
A_0	area of array receiving zero order light, m^2
A_1	area of array receiving first- and second-order light, m^2
a^i	area of array composed of semiconductor group i, m^2
B	q/bT, V^{-1}
b	Boltzmann constant, $J/^oK$
C	constant of proportionality
c	velocity of light, m/sec
D_0^i	material constant of semiconductor group i, $(m^{-6})(^oK^{-3})$
d	groove width of grating, μm
E_{BG}^i	band gap energy of group i, eV
f	weight per unit A_m/weight per unit A
H	spectral irradiance, $W/(m^2)(\mu m)$
h	Planck constant, (J)(sec)
I	intensity, W/m^2
i	superscript indicating semiconductor group i

$J^i_{s,k}$	short-circuit current density from group i in array at order k, A/m^2
J^i_0	reverse saturation current density, A/m^2
k	index indicating diffraction order
L, 1	index indicating diffraction order
M	total number of grooves in grating
N_A	acceptor density in p region of semiconductor, m^{-3}
N_D	donor density in n region of semiconductor, m^{-3}
n_{ph}	photon flux, photons/(m^2)(sec)
P_a	incident power absorbed by array, W
$P_{a,k}$	incident power absorbed by array receiving light from order k, W
P_m	output power from array, W
$P_{m,k}$	output power from array receiving light from order k, W
p	number of surfaces in optical system
Q	collection efficiency of p-n junction
q	electron charge, C
R	reflection coefficient of semiconductor surface
RPW	relative power-to-weight ratio
r	reflection coefficient of surfaces in optical system
T	temperature of array, ^oK
t	temperature of array, ^oC
$V_{m,k}$	voltage at maximum power, V
x	thickness of solar cells, m
α	$\pi d \sin \theta/\lambda$
β	$\pi d/\lambda(\sin \theta + \tan \delta(1 + \cos \theta))$
γ	absorption coefficient of semiconductor material, m^{-1}
δ	angle formed by normal to groove surface and grating plane
ϵ	emissivity of array surface
η_{DLS}	conversion efficiency of dispersed light system
η_{GA}	conversion efficiency of gallium arsenide array

η_g	grating efficiency
θ	angle of diffraction
Λ	relative wavelength λ/λ_B
λ	wavelength, μm
λ_B	blaze wavelength of grating, μm
λ_{BG}^i	band gap wavelength of group i, μm
λ_{max}	maximum wavelength considered in spectrum of sun, μm
λ_{min}	minimum wavelength considered in spectrum of sun, μm
μ_n	mobility of electrons, $m^2/(V)(sec)$
μ_p	mobility of holes, $m^2/(V)(sec)$
σ	Stefan-Boltzmann constant, $W/(m^2)(^oK^4)$
τ_n	lifetime of electrons, sec
τ_p	lifetime of holes, sec

SYSTEM ASSUMPTIONS AND ANALYSIS

The essential features of two ideal dispersed light systems are illustrated in figure 1. The actual arrangement and number of auxiliary optical components necessary to focus the dispersed beam onto the array depends primarily on the geometry and the operation of the diffraction grating. Concave gratings, in the Rowland circle (ref. 4) arrangement, for example, do not need additional optics to focus the diffracted beam provided the focal point of the concentrator, the solar cell array, and the grating itself all lie on the circumference of a circle having a radius equal to one-half the radius of the grating. On the other hand, the plane diffraction grating requires two additional mirrors; one to collimate the light incident upon its face, and a second to focus the diffracted beam onto the array. System configurations other than the two described herein are possible but will not be considered since they are basically variations in arrangements of the gratings and mirrors previously described.

In order to obtain results which are a measure of the upper limit efficiencies of the dispersed light system, three assumptions regarding the system were made:

(1) The sunlight incident upon the concentrating mirror has a wavefront which is plane and parallel to the projected area of the mirror.

(2) The optical elements undergo no mechanical distortion.

(3) The diffracted light is perfectly focused on the array.

The conventional array which is to be compared with the dispersed light system is an array of single band gap photovoltaic cells, all of one semiconductor material, arranged on a flat plate normal to the sun. Gallium arsenide, which has been shown to provide optimum theoretical conversion efficiency under sunlight, is the semiconductor material employed in the planar array for this study (ref. 1).

The performance parameters, efficiency, power-to-weight ratio, and array temperature, for either system were computed with the assumption that heat produced by the interaction of photons and solar cells is radiated passively from both front and back surfaces of the array. Thus, according to the thermal balance equation,

$$P_a - P_m = 2\sigma\epsilon T^4 A \tag{1}$$

where P_a is the power absorbed by the array, P_m is the output power from the array, A is array area, T is array temperature, ϵ is the surface emissivity, and σ is the Stefan-Boltzmann constant. In this analysis, ϵ is assumed to be equal to 1 for all array surfaces.

POWER INCIDENT ON ARRAY, DIFFRACTION GRATINGS

In equation (1), the input power is the energy absorbed by the array in unit time. For the planar array, this power input is simply the product of absorbed sunlight intensity and array area. The situation in the case of dispersed light arrays is not as straightforward because of the properties of diffraction gratings and of the variety of semiconductor materials employed. Unlike a prism, which directs its dispersed beam in one general direction, a diffraction grating necessarily sends dispersed beams into several angular regions, called diffraction orders. Since both the direction and the amount of energy contained in each dispersed beam are important to the placement and spectrum match of the array or arrays, a brief analysis of gratings will be undertaken at this point.

When maximum intensity in one diffraction order is desirable, as it is in dispersion arrays, gratings are ruled by a technique called blazing; groove facets are so cut at a predetermined angle to the grating surface that as much energy as possible is directed into the desired region. The equations for the intensity of blazed gratings have been derived elsewhere (ref. 5). For light incident normal to the surface of the blazed grating, the equation becomes

$$I(\lambda) = C\left\{\left[\cos\delta + \cos(\delta + \theta)\right]^2 \cos^2\theta\right\} \frac{\sin^2\beta}{\beta^2} \frac{\sin^2 M\alpha}{\sin^2\alpha} \tag{2}$$

$$\alpha = \frac{\pi d \sin \theta}{\lambda} \tag{3a}$$

$$\beta = \frac{\pi d}{\lambda}\left[\sin \theta + (\tan \delta)(1 + \cos \theta)\right] \tag{3b}$$

where M is the number of grooves cut in the grating, λ is the wavelength of light diffracted at angle θ from a grating of groove width d, δ is the angle made by the normals of groove surface and grating plane, and C is a proportionality constant. Figure 2 illustrates a profile of a plane blazed grating as well as the physical parameters previously described.

The intensity from a diffraction grating at any wavelength and diffraction angle is a product of three mutually dependent functions which may be analyzed individually to describe the distribution of energy among the diffraction orders. The most important terms, the interference function $\sin^2 M\alpha / \sin^2 \alpha$ and the diffraction function $\sin^2 \beta / \beta^2$ will be reviewed briefly. The geometric term involving cosines of δ and θ does affect the intensity somewhat but is less complicated and less important and will not be analyzed in this report. The interference function determines the conditions under which light waves, reflected from M grooves, constructively interfere to produce intensity

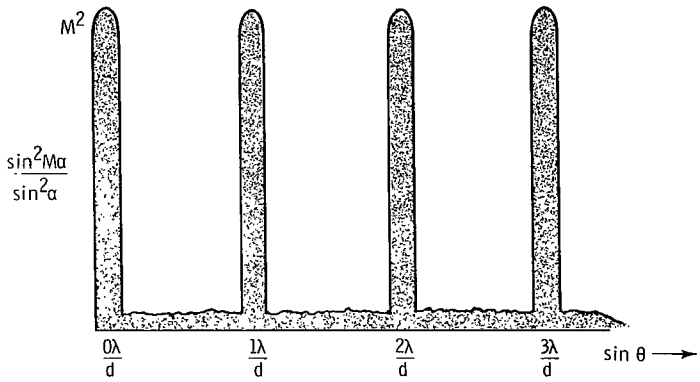

maximums. Because of rapid variation of $\sin M\alpha$ relative to $\sin \alpha$, this function has a sharp rise from zero intensity to maximum intensity proportional to M^2 for a given λ whenever $\alpha = k\pi$, or

$$\sin \theta_k = \frac{k\lambda}{d} \qquad k = 0,\ 1,\ 2,\ \ldots \tag{4}$$

Thus, the interference function gives rise to the concept of diffraction orders previously described and, as shown in the sketch, the intensity is a constant for all λ and k under the effects of interference alone. The intensity distribution of a grating, however, is not

a constant because of the modulating influence of the diffraction function $\sin^2\beta/\beta^2$. Unlike the interference term, the diffraction function has only one maximum in each order, which occurs when $\beta = 0$ and is determined by d, δ, and λ. Thus, if a maximum intensity is desired for a given order and wavelength, called the blaze wavelength λ_B, the grating must be so fabricated that $\beta = 0$ in equation (3b). Since there is only one condition for which $\sin^2\beta/\beta^2$ is a maximum in any order, the intensity from a grating at wavelengths other than the blaze wavelength will be less than optimum. The result is that no single diffraction order will contain the total incident energy within its dispersed beam.

Several general features of blazed gratings which affect the input and the output powers in equation (1) may be observed from investigation of the diffraction equations. When $k = 0$, $\sin\theta$ is zero for all wavelengths; there is no chromatic dispersion in the zero order. Consequently, to convert the energy in this order, the dispersed-light system must employ an additional array composed of only one semiconductor material to absorb photons of all energies in the zero order. The result is that this portion operates only as efficiently as a conventional array. Another important property is that diffraction orders for k greater than zero do not separate into distinct dispersion spectra but overlap one another subject to the condition $k\lambda/d$ is equal to a constant (see eq. (4)). Since dispersed-light systems operate by a spectrum match between band gap and photon energy, minimum spectral mismatch is obtained by positioning the array to receive the first-order diffraction spectrum. Nevertheless, the unavoidable overlap in orders will result in the absorption of photons with energies twice and three times the band gap energy by some portions of the dispersion array; the efficiency of the array is consequently diminished.

The grating equation (eq. (4)) provides the information concerning the proportion of array area associated with each material band gap. The dispersion angle between any two wavelengths may be obtained by differentiating equation (4) and thereby obtaining the relation $d\theta = kd\lambda/d\cos\theta_k$. For small angles of dispersion, the variation in $\cos\theta_k$ can be neglected, and the angular deviation between two wavelengths is proportional to the difference in wavelength. With the assumptions stated earlier in this analysis, Beutler (ref. 6) has shown that the distance between any two wavelengths in the focal plane of the Rowland circle is proportional to the difference in diffraction angle and, hence, to the wavelength difference. Likewise in the case of the plane grating and the parabolic focus mirror, the distance between any two wavelengths in the focal plane of the parabola may be shown to be proportional to the wavelength difference. Of course, the dispersion angle from the grating and the deviation of incidence angle from the optic axis of the parabola must be kept small. Hence, under conditions of perfect focusing in either grating configuration, the fraction of total array area alloted to a group of cells of band gap wavelength λ_{BG}^{i} is

$$\frac{a^i}{A_1} = \frac{\lambda_{BG}^i - \lambda_{BG}^{i+1}}{\lambda_{max} - \lambda_{min}} \tag{5}$$

where a^i is the area of cells with band gap wavelength λ_{BG}^i, A is panel area receiving light in the wavelength range λ_{min} to λ_{max}, λ_{BG}^{i+1} is the wavelength associated with band gap of next material used in the array.

The proportion of total energy of a given wavelength going into order k is then given by

$$\eta_g(\lambda, k) = \frac{I(\lambda, k)\cos\theta_k}{\sum_{l=0}^{\pm L} I(\lambda, l)\cos\theta_l} \tag{6}$$

where $\eta_g(\lambda, k)$ will be called the grating efficiency in order k, and L is the number of diffraction orders on either side of the zero order. Since $\eta_g(\lambda, k)$ gives the fraction of incident photon flux of given wavelength in any order k, the grating efficiency will prove useful in calculation of the electric carriers produced in a p-n junction. Grating efficiency for the zero, first, and second orders were therefore computed as a function of wavelength for several blaze wavelengths and groove widths. Curves of grating efficiency as a function of relative wavelength λ/λ_B and groove width d are plotted in figure 3. The range of d considered represents a wide variation in dispersion angle over the white light spectrum (0.3 to 1.5 μm), as may be seen from equation (4). Hence, since the efficiency does not change much with changes in groove width, a groove width of 5 microns shall be used in further calculations.

It is now possible to determine the power which will impinge upon the surface of any group i of solar cells in the array.

The power incident on a solar cell group i in the array positioned to receive light from the first diffraction order is

$$P_{a,1}^i = A_m r^p \left[\int_{\lambda_{BG}^{i+1}}^{\lambda_{BG}^i} n_{ph}(\lambda)\eta_g(\lambda, 1)\frac{hc}{\lambda}\,d\lambda + \int_{\lambda_{BG}^{i+1}/2}^{\lambda_{BG}^i/2} n_{ph}(\lambda)\eta_g(\lambda, 2)\frac{hc}{\lambda}\,d\lambda \right] \tag{7a}$$

while the power incident on the group receiving light from the zero diffraction order is

$$P_{a,0} = A_m r^p \int_{\lambda_{min}}^{\lambda_{max}} n_{ph}(\lambda)\eta_g(\lambda, 0)\frac{hc}{\lambda}\,d\lambda \tag{7b}$$

where A_m is the projected concentrator area, r is the specular reflection coefficient of each of the p optical components, $n_{ph}(\lambda)$ is the photon flux from the sun at wavelength λ, and hc/λ is the energy per photon. The cell group with wavelength λ_{BG}^{i+1} situated next to area a^i is the cutoff point for group i.

POWER OUTPUT FROM ARRAYS, p-n JUNCTION OPERATION

The equation for incident power on any portion of the dispersion array has been demonstrated; the output power of that portion will now be investigated. The theory of ideal p-n junction has been presented elsewhere, and only a brief review of pertinent equations will be given here (refs. 7 to 9). The maximum power available from an ideal p-n junction photovoltaic area a^i is given by

$$P_{m,k}^i = J_{s,k}^i \left[\frac{B\left(V_{m,k}^i\right)^2}{1 + BV_{m,k}^i}\right] a^i$$

where $B = q/bT$, $J_{s,k}^i$ is the short-circuit current density, and $V_{m,k}^i$ is the maximum power voltage and is related to $J_{s,k}^i$ by the equation:

$$e^{BV_{m,k}^i}\left(1 + BV_{m,k}^i\right) = \frac{J_{s,k}^i}{J_0^i} + 1 \tag{8}$$

The term J_0^i in the previous equation is called the reverse saturation current density and is dependent upon semiconductor material parameter and temperature of the cells. This term is given by

$$J_0^i = D_0^i q T^3 e^{-qE_{BG}^i/bT}\left[\frac{1}{N_A}\left(\frac{\mu_n}{\tau_n}\frac{bT}{q}\right)^{1/2} + \frac{1}{N_D}\left(\frac{\mu_n}{\tau_p}\frac{bT}{q}\right)^{1/2}\right] \tag{9}$$

where D_0^i is a constant of semiconductor i, T is the temperature, E_{BG}^i is the band gap energy, μ_n is electron mobility, μ_p is hole mobility, τ_p is hole lifetime, N_A is density in p region, N_D is donor density in n region. On the other hand, $J_{s,k}^i$ is not strongly temperature sensitive but is a function of the flux of photons which are absorbed by the cell and result in a current carrier flow through an external load. The equation for $J_{s,1}^i$ after diffraction and absorption of light within the cell group i is

$$J_{s,1}^i = \frac{A_m}{a^i} r^p \left\{ \int_{\lambda_{BG}^{i+1}}^{\lambda_{BG}^i} qn_{ph}(\lambda)\eta_g(\lambda, 1)\left[1 - R(\lambda)\right]\left[1 - e^{-\gamma(\lambda)x}\right]Q(\lambda)d\lambda \right.$$

$$\left. + \int_{\lambda_{BG}^{i+1}/2}^{\lambda_{BG}^i/2} qn_{ph}(\lambda)\eta_g(\lambda, 2)\left[1 - R(\lambda)\right]\left[1 - e^{-\gamma(\lambda)x}\right]Q(\lambda)d\lambda \right\} \qquad (10)$$

where $1 - R(\lambda)$ is the transmission efficiency through the front surface of the cell, $1 - e^{-\gamma(\lambda)x}$ is the absorption efficiency within the cell, and $Q(\lambda)$ is the collection efficiency or the fraction of generated current carriers which flow through the external load. All other terms and symbols have been previously described. The last three efficiencies stated are functions of the physical properties of the cell and in calculations of optimum conversion efficiencies are assumed to be equal to 1 (ref. 1).

The output power, then, of the solar cell group i positioned to receive the chromatically dispersed light is

$$P_{m,1}^i = A_m r^p \left[\int_{\lambda_{BG}^{i+1}}^{\lambda_{BG}^i} qn_{ph}(\lambda)\eta_g(\lambda, 1)d\lambda + \int_{\lambda_{BG}^{i+1}/2}^{\lambda_{BG}^i/2} qn_{ph}(\lambda)\eta_g(\lambda, 2)d\lambda \right] \frac{B\left(V_{m,1}^i\right)^2}{1 + BV_{m,1}^i} \qquad (11a)$$

Likewise, the output power of an array made up of only one type of semiconductor material receiving nondispersed light is

$$P_{m,0} = A_m r^p \left[\int_{\lambda_{min}}^{\lambda_{BG}} qn_{ph}(\lambda)\eta_g(\lambda, 0)d\lambda \right] \frac{B\left(V_{m,0}\right)^2}{1 + BV_{m,0}} \qquad (11b)$$

This expression may be used to calculate the power out of the zero order of the dispersion system; it may also be used to calculate the output power for an ordinary planar array under the condition that

$$p = 0$$

and

$$\eta_g(\lambda, 0) = 1$$

The power balance equation (1) for the dispersion array made up of spectrally matched areas placed laterally to receive the dispersed beam focused upon the array surface then becomes

$$\left(P_{a,0} + \sum_{i=1}^{6} P_{a,1}^{i}\right) - \left(P_{m,0} + \sum_{i=1}^{6} P_{m,1}^{i}\right) = 2\sigma\epsilon T^4 (A_0 + A_1) \tag{12}$$

The conversion efficiency of the system then can be calculated from the equation

$$\eta_{DLS} = \frac{P_{m,0} + \sum_{i=1}^{6} P_{m,1}^{i}}{(1350 A_m)} \tag{13}$$

where 1350 watts per square meter is the total intensity incident upon the concentrating mirror surface.

APPLICATION OF ANALYSIS

The variation with temperature of output power for the dispersed-light system was calculated on a digital computer with equations (6) to (12). The necessity of considering the performance over a range of temperature arises from the fact that the concentration ratio $A_m/(A_1 + A_0)$ of the dispersed light system is not fixed by outside constraints. Thus, unlike the conventional array, which has a temperature and output power determined by array properties and distance from the sun, the dispersed-light system performance is influenced by the concentration ratio as well. In this analysis, then, iteration about each temperature point involves the application of the appropriate concentration ratio in the power terms of equation (12). The photon flux from the sun used in the analysis was obtained from data published by Johnson and listed in table I (ref. 10); the flux

may be calculated from the table simply by dividing the spectral irradiance at λ by the energy per photon. Similarly, the list of photovoltaic semiconductors and their material properties in table II are from previous work on p-n junctions (refs. 1 and 11). The semiconductors included in the list are only those which have been or are being investigated for possible development as power producing solar cells.

With the above information, then, the energy conversion efficiency as a function of temperature was computed for several different grating and surface conditions of the dispersed light system. The cases considered are as follows:

(1) Upper limit conversion efficiency: This is the optimum efficiency available from the array listed in table II since this efficiency is based upon zero reflection loss and the optimistic assumption that all the energy is diffracted into the first order.

(2) Conversion efficiency with grating losses only: In this case, the conversion efficiency of the dispersed light system includes the effect of loss due to grating efficiency, calculated from equation (5) for several blaze wavelengths over the range 0.3 to 1 micron. These grating losses were studied as a function of both blaze wavelength and temperature. A family of curves of conversion efficiency against blaze wavelength, with temperature as a parameter, was computed, and the optimum grating condition was selected for use in further calculations.

(3) Conversion efficiency under grating and surface reflection losses: Here, the optimum grating efficiency and the reflection losses from each optical surface of the dispersed light system were combined to obtain an estimate of the energy conversion efficiency or a function of temperature for each system configuration. The reflection coefficient from each of the p optical components in either optical system was assumed to be equal to 0.9.

For comparison with the dispersed light system, the conversion efficiency and operating temperature of the GaAs array were also calculated using equations (6) to (12). The photon flux and the material parameters used were also obtained from tables I and II. The basic difference in the calculation, of course, was that equation (12) was solved for only one temperature point and one concentration ratio.

RESULTS AND DISCUSSION

System Efficiency

Results of the analysis for the systems studied are given in figures 4 to 7. Figure 4 illustrates the dispersed light system conversion efficiency as a function of blaze wavelength and temperature. The curves, obtained by applying equations (10) to (13) under conditions of zero reflection losses from the optical surfaces, present the effects of the

grating and of the solar cell materials on the performance of the system and demonstrate the blaze condition necessary for optimum conversion efficiency. Maximum efficiency occurs at a blaze wavelength of about 0.6 micron. With a 0.3-micron change of wavelength on either side of the optimum blaze wavelength, the efficiency falls to about 75 percent of maximum. Further, the change of efficiency with temperature is not wavelength dependent as can be seen from the uniform distance between curves.

The optimum blaze condition is the result of a compromise between energy losses into the zero diffraction order on the one hand and losses into higher orders than the first on the other. The loss of conversion efficiency at low blaze wavelength is due to the fact that a high proportion of the energy is diffracted into the zero order. The solar cells which receive light from the zero order are all one band gap and convert the light energy no more efficiently than the conventional type of solar cell array. Similarly, when the grating is blazed for longer wavelengths, a great proportion of energy falls into the second diffraction order. The result, here, is that high-energy photons of the second order overlap low-energy regions of the first order. Since the solar cells in that region are designed to convert low-energy photons most efficiently, the mismatch in energy is dissipated in the solar cells as heat. Thus, the optimum blaze condition in figure 4 represents the case for which minimum energy losses occur in the zero and second diffraction orders.

Figure 5 demonstrates the conversion efficiencies of the concave configuration over the temperature range of 0° to 150° C under various energy loss conditions. For comparison, the conversion efficiency and operating temperature of the GaAs array at 1 solar constant intensity is also shown in the figure. The upper limit conversion efficiency of the dispersed light system exhibits a significant increase of about 1.2 to 1.8 times greater throughout the range of temperatures considered over the efficiency (26 percent) of the GaAs array. Grating diffraction losses even under optimum grating conditions, however, reduce the conversion efficiency by 6 percent. Surface reflection losses from the optical components in the concave configuration account for a further decrease in efficiency of 7 percent. For the plane grating configuration the decrease in efficiency is another 7 percent because of losses from two additional mirror surfaces. The result of these losses may be seen in figure 6, where the concave grating configuration, plane grating configuration, and the GaAs array are compared. The plane grating configuration exhibits no advantage in efficiency over the GaAs array; while there is some advantage afforded by the concave configuration, the difference in conversion efficiency between that system and the GaAs array is about 4 to 6 percent.

Power-to-Weight Ratio

When weight is a factor in launching a vehicle into space, the relative power-to-

weight ratio between two competing solar cell systems is an important criterion for comparison of systems. In this analysis, the relative power-to-weight ratio RPW between the dispersed light system and the GaAs array has been calculated by the relation:

$$RPW = \frac{\eta_{DLS}}{\eta_{GA}} \frac{1}{\frac{A_0 + A_1}{A_m} + f}$$

where f is the weight per unit concentrator area divided by weight per unit array area. Values of conversion efficiency from figure 6 were used to plot the RPW for the concave configuration in figure 7 as a function of temperature (and concentration ratio, $A_m/A_0 + A_1$), with f as a parameter. It is seen from figure 7 that relative power-to-weight ratio increases with temperature and concentration ratio. Thus, since η_{DLS} has been shown in figure 6 to decrease with temperature and to offer small advantage only at the low temperature, the increase in RPW with temperature is due mainly to increased concentration ratio. Figure 7 further illustrates the effect of concentration ratio on the RPW of the concave configuration by the fact that the dispersed light system requires the use of lightweight concentration mirrors. The dispersed light system does not begin to have an advantageous RPW until the area density of the concentrator is about one-half the area density of the solar cell array.

SUMMARY OF RESULTS

An analysis of a dispersed light system utilizing an array of photovoltaic materials arranged to match the spectral output of an optical system composed of concentrating mirror and diffraction gratings has been made to obtain an estimate of performance parameters of the system relative to an ordinary planar array. The conditions of analysis were generally optimistic for the dispersion array; it was assumed that collimated sunlight, incident upon the concentrating mirror, was perfectly focused by the optical system onto the photovoltaic array.

The theoretical conversion efficiency of the dispersed light system under no diffraction or reflection losses was found to be 1.2 to 1.8 times the efficiency of a conventional type gallium arsenide (GaAs) array (26 percent) throughout the range of temperatures considered (0° to 150° C operating temperatures of dispersed light system array). When diffraction and reflection losses were included, however, the conversion efficiency of the dispersed light system was considerably diminished. The plane grating configuration showed no advantage in efficiency over the conventional array, while the concave grating configuration exhibited some advantage. The difference in efficiency between the latter

configuration and the GaAs array was 4 to 6 percent in the low-temperature region (0° to 90° C).

Comparison of power-to-weight ratios between the dispersed light system and the gallium arsenide array demonstrates the necessity of high concentration ratios and lightweight mirror if the dispersed light system were to compete successfully with a conventional array. The power-to-weight ratio of the dispersed light system tends to increase with temperature, even though power output decreases with temperature. The increase in power-to-weight ratio, then, is a result of the higher concentration ratios available at higher temperature. To have an advantage in power-to-weight ratio, though, the dispersed light system must utilize lightweight concentrating mirrors. Based only on limited energy losses, the concentrator weight per unit area must be one-half the array weight per unit area in order to show a power-to-weight advantage for the dispersed light system.

Lewis Research Center,
National Aeronautics and Space Administration,
Cleveland, Ohio, April 10, 1967,
120-33-01-10-22.

REFERENCES

1. Wysocki, Joseph J.; and Rappaport, Paul: Effect of Temperature on Photovoltaic Solar Energy Conversion. J. Appl. Phys., vol. 31, no. 3, Mar. 1960, pp. 571-578.

2. Jackson, E. D.: Areas for Improvement of the Semiconductor Solar Energy Converter. Electrical Processes. Vol. 5 of the International Conference on the Use of Solar Energy - The Scientific Basis, Tucson, Oct. 31-Nov. 1, 1955. University of Arizona Press, 1958, pp. 122-126.

3. Ratajczak, Anthony F.: Theoretical Performance of Solar-Cell Space Power Systems Using Spectral Dispersion. I - Dispersion by Prism Reflector. NASA TN D-4156, 1967.

4. Born, Max; and Wolf, Emil: Principles of Optics. Pergamon Press, 1959.

5. Barrekette, E. S.; and Christensen, R. L.: On Plane Blazed Gratings. I.B.M. J. Res. and Develop., vol. 9, no. 2, Mar. 1965, pp. 108-117.

6. Beutler, H. G.: The Theory of the Concave Grating. J. Opt. Soc. Am., vol. 35, no. 5, May 1945, pp. 311-350.

7. Shockley, William: Electrons and Holes in Semiconductors. D. Van Nostrand Co., Inc., 1950.

8. Cummerow, Robert L.: Photovoltaic Effect in P-N Junctions. Phys. Rev., vol. 95, no. 1, July 1, 1954, pp. 16-21.

9. Moss, T. S.: The Potentialities of Silicon and Gallium Arsenide Solar Batteries. Solid State Electronics, vol. 2, no. 4, May 1961, pp. 222-231.

10. Johnson, Francis S.: The Solar Constant. J. Meteorol., vol. 11, no. 6, Dec. 1954, pp. 431-439.

11. Groves, W. O.; and Epstein, A. S.: Development of Improved Single Crystal Gallium Phosphide Solar Cells. Monsanto Research Corp. (NASA CR-54273), 1964.

TABLE I. - SOLAR SPECTRAL IRRADIANCE DATA

Wavelength, λ, μm	Mean zero air mass spectral irradiance, H, $W/(cm^2)(\mu m)$	Solar constant associated with wavelength shorter than wavelength P_λ, percent	Wavelength, λ, μm	Mean zero air mass spectral irradiance, H, $W/(cm^2)(\mu m)$	Solar constant associated with wavelength shorter than wavelength P_λ, percent	Wavelength, λ, μm	Mean zero air mass spectral irradiance, H, $W/(cm^2)(\mu m)$	Solar constant associated with wavelength shorter than wavelength P_λ, percent	Wavelength, λ, μm	Mean zero air mass spectral irradiance, H, $W/(cm^2)(\mu m)$	Solar constant associated with wavelength shorter than wavelength P_λ, percent
0.22	0.0030	0.02	0.36	0.116	5.47	0.50	0.198	23.5	0.68	0.151	46.7
.225	.0042	.03	.365	.129	5.89	.505	.197	24.2	.69	.148	17.8
.23	.0052	.05	.37	.133	6.36	.51	.196	24.9	.70	.144	48.8
.235	.0054	.07	.375	.132	6.84	.515	.189	25.6	.71	.141	49.8
.24	.0058	.09	.38	.123	7.29	.52	.187	26.3	.72	.137	50.3
.245	.0064	.11	.385	.115	7.72	.525	.192	26.9	.73	.134	51.8
.25	.0064	.13	.39	.112	8.13	.53	.195	27.6	.74	.130	52.7
.255	.010	.16	.395	.120	8.54	.535	.197	28.3	.75	.127	53.7
.26	.013	.20	.40	.154	9.03	.54	.198	29.0	.80	.1127	57.9
.265	.020	.27	.405	.188	9.65	.545	.198	29.8	.85	.1003	61.7
.27	.025	.34	.41	.194	10.3	.55	.195	30.5	.90	.0895	65.1
.275	.022	.43	.415	.192	11.0	.555	.192	31.2	.95	.0803	68.1
.28	.024	.51	.42	.192	11.7	.56	.190	31.8	1.0	.0725	70.9
.285	.034	.62	.425	.189	12.4	.565	.189	32.5	1.1	.0606	75.7
.29	.052	.77	.43	.178	13.0	.57	.187	33.2	1.2	.0501	79.6
.295	.063	.98	.435	.182	13.7	.575	.187	33.9	1.3	.0406	82.9
.30	.061	1.23	.44	.203	14.4	.58	.187	34.5	1.4	.0328	85.5
.305	.067	1.43	.445	.215	15.1	.585	.185	35.2	1.5	.0267	87.6
.31	.076	1.69	.45	.220	15.9	.59	.184	35.9	1.6	.0220	89.4
.315	.082	1.97	.455	.219	16.7	.595	.183	36.5	1.7	.0182	90.83
.32	.085	2.26	.46	.216	17.5	.60	.181	37.2	1.8	.0152	92.03
.325	.102	2.60	.465	.215	18.2	.61	.177	38.4	1.9	.01274	93.02
.33	.115	3.02	.47	.217	19.0	.62	.174	39.7	2.0	.01079	93.87
.335	.111	3.40	.475	.220	19.8	.63	.170	40.9	2.1	.00917	94.58
.34	.111	3.80	.48	.216	20.6	.64	.166	42.1	2.2	.00785	95.20
.345	.117	4.21	.485	.203	21.3	.65	.162	43.3	2.3	.00676	95.71
.35	.118	4.63	.49	.199	22.0	.66	.159	44.5	2.4	.00585	96.18
.355	.116	5.04	.495	.204	22.8	.67	.155	45.6	2.5	.00509	96.57

TABLE II. - SEMICONDUCTORS AND MATERIAL PROPERTIES USED IN ANALYSIS

[Density in p-region N_A, 5×10^{18} atoms/cm^3; donor density in n-region N_D, 1×10^{17} atoms/cm^3.]

Semiconductor	Mobility		Lifetime		Band gap energy, E^i_{BG}, eV	Band gap temperature coefficient, $\Delta E^i_{BG}/\Delta T$, eV/^oK	Material constant, D^i_0, $(m^{-6})(^oK^{-3})$
	Electron, μ_n, $m^2/(V)(sec)$	Hole, μ_p, $m^2/(V)(sec)$	Electron, τ_n, sec	Hole, τ_p, sec			
Germanium	0.3000	0.1350	10^{-6}	10^{-5}	0.83	-0.0004	3.7×10^{42}
Silicon	.0710	.0360	10^{-7}	10^{-6}	1.20	.00035	2.23×10^{43}
Indium phosphide	.4000	.0100	10^{-8}	10^{-7}	1.39	.0004	4.46×10^{41}
Gallium arsenide	.5000	.0400	↓	↓	1.50	.0005	1.82×10^{41}
Cadmium telluride	.0300	.0100	↓	↓	1.57	.0004	2.23×10^{43}
Gallium arsenide phosphide $GaAs_{1-x}P_x$	.0200	.0020	↓	↓	1.90 to 2.20	.0004	2.23×10^{43}

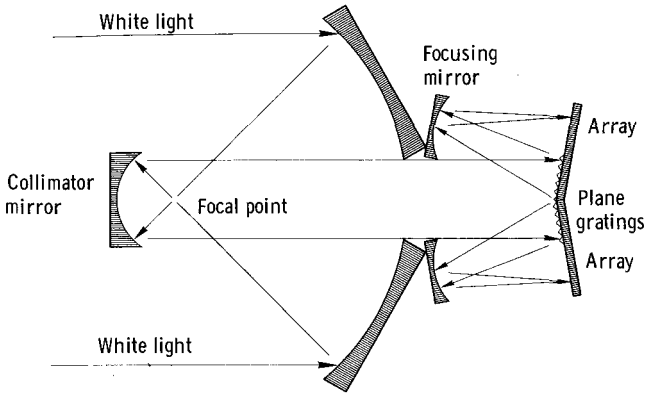

(a) Plane.

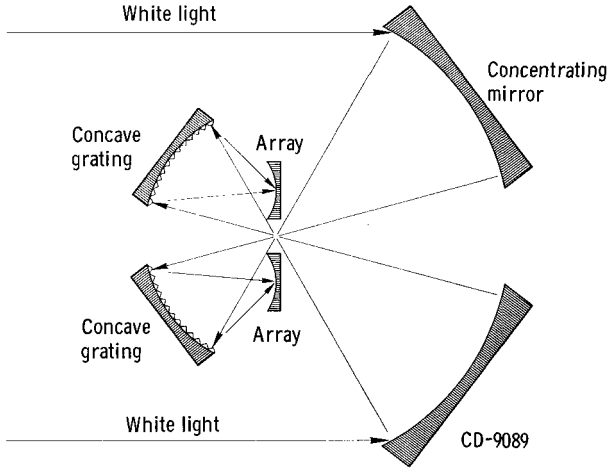

(b) Concave.

Figure 1. - Grating configurations.

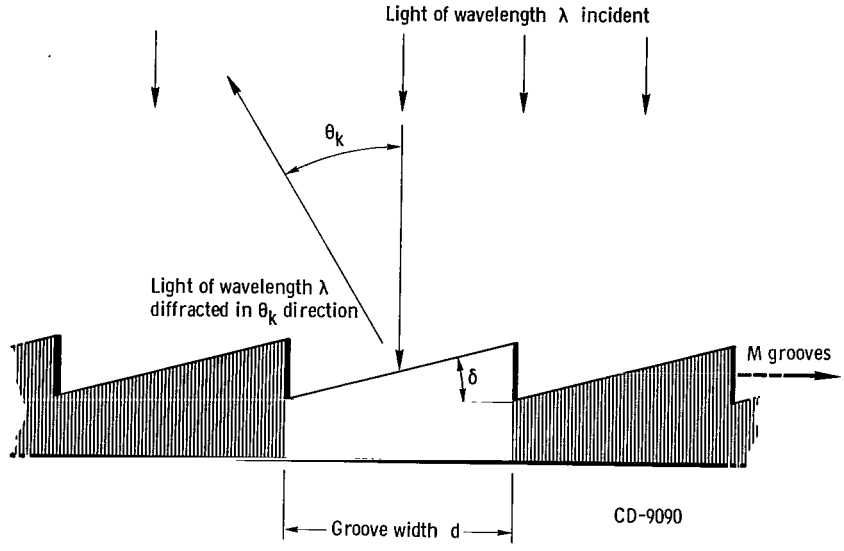

Figure 2. - Cross section of diffraction grating.

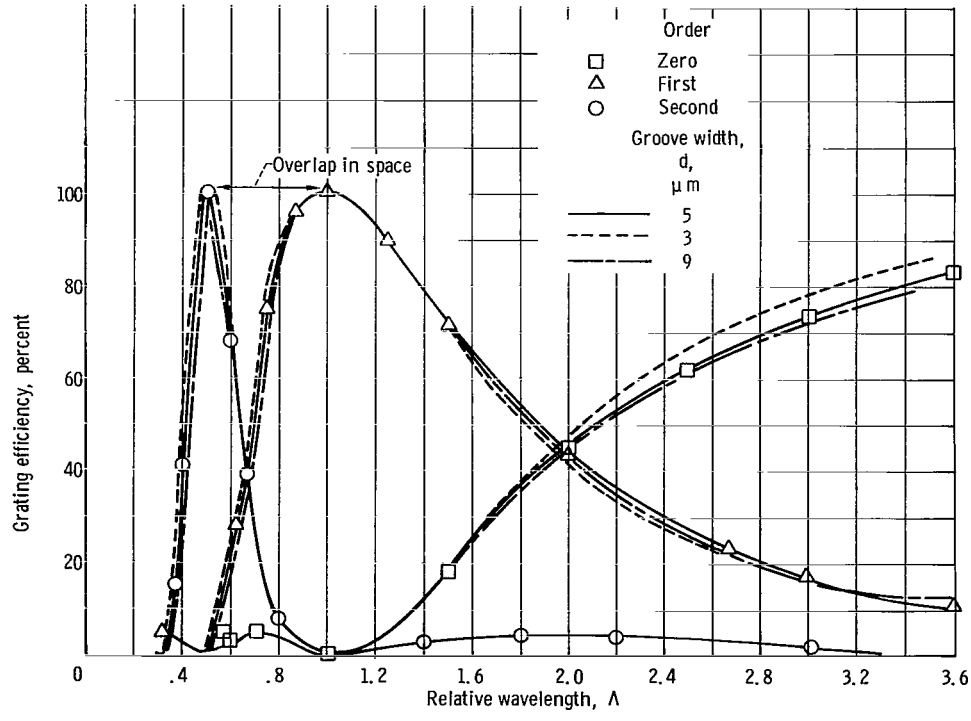

Figure 3. - Effect of relative wavelength on grating efficiency.

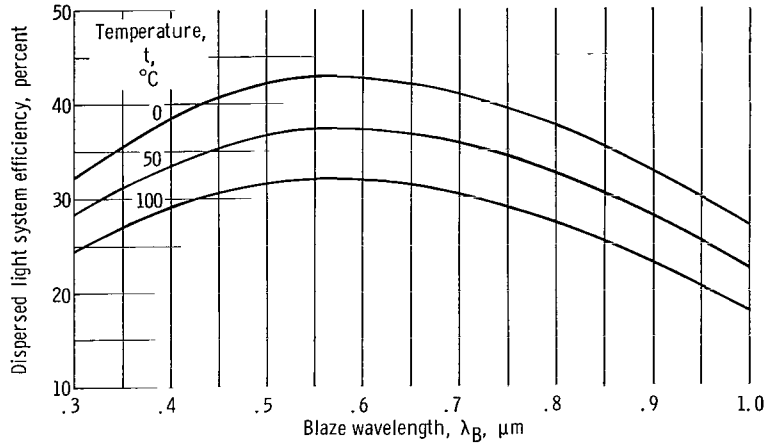

Figure 4. - Effect of blaze wavelength and temperature on dispersed light system efficiency. Reflection loss equal to zero.

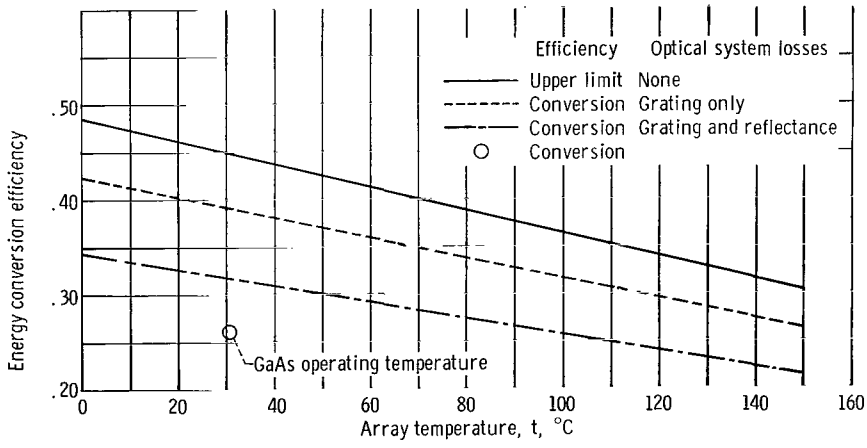

Figure 5. - Comparison of concave configuration efficiency with various system conditions.

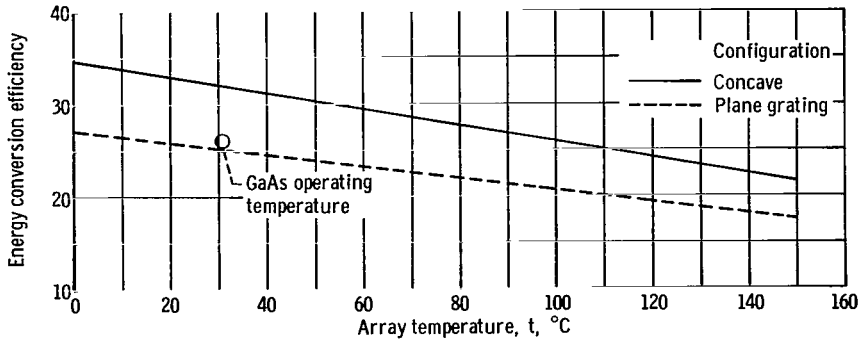

Figure 6. - Comparison of concave and plane grating configuration efficiencies with GaAs array efficiency.

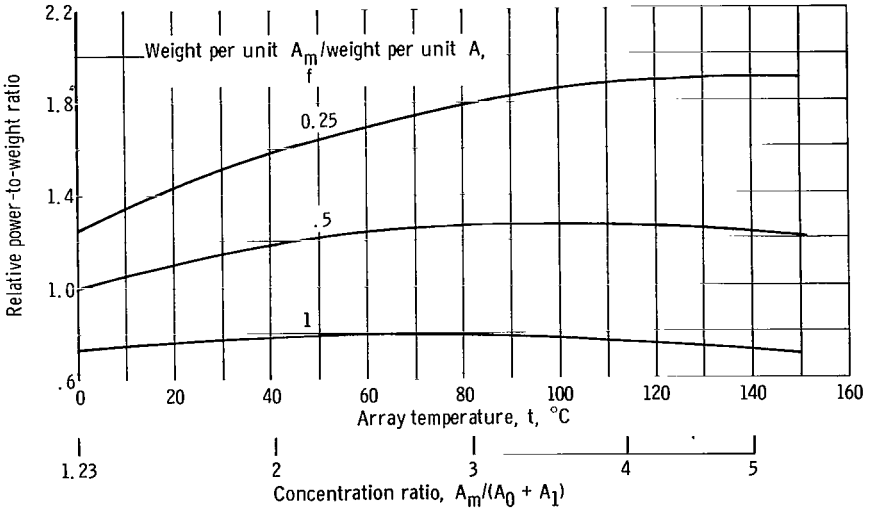

Figure 7. - Relative power-to-weight ratio of dispersed light system to gallium arsenide array.

"The aeronautical and space activities of the United States shall be conducted so as to contribute . . . to the expansion of human knowledge of phenomena in the atmosphere and space. The Administration shall provide for the widest practicable and appropriate dissemination of information concerning its activities and the results thereof."

—NATIONAL AERONAUTICS AND SPACE ACT OF 1958

NASA SCIENTIFIC AND TECHNICAL PUBLICATIONS

TECHNICAL REPORTS: Scientific and technical information considered important, complete, and a lasting contribution to existing knowledge.

TECHNICAL NOTES: Information less broad in scope but nevertheless of importance as a contribution to existing knowledge.

TECHNICAL MEMORANDUMS: Information receiving limited distribution because of preliminary data, security classification, or other reasons.

CONTRACTOR REPORTS: Scientific and technical information generated under a NASA contract or grant and considered an important contribution to existing knowledge.

TECHNICAL TRANSLATIONS: Information published in a foreign language considered to merit NASA distribution in English.

SPECIAL PUBLICATIONS: Information derived from or of value to NASA activities. Publications include conference proceedings, monographs, data compilations, handbooks, sourcebooks, and special bibliographies.

TECHNOLOGY UTILIZATION PUBLICATIONS: Information on technology used by NASA that may be of particular interest in commercial and other non-aerospace applications. Publications include Tech Briefs, Technology Utilization Reports and Notes, and Technology Surveys.

Details on the availability of these publications may be obtained from:

SCIENTIFIC AND TECHNICAL INFORMATION DIVISION

NATIONAL AERONAUTICS AND SPACE ADMINISTRATION

Washington, D.C. 20546